A SVM Control Scheme for Impedance Source Inverter-Based Wind Driven SEIG Fed Motor Drives

Max SAVIO. F Vasantharaj S
PG Scholar, Jeppiaar Engineering College, Chennai, India
msavio19@gmail.com vasantharaj118@gmail.co
Sasikumar M
Professor & Head, Jeppiaar Engineering College, Chennai. India
pmsasi77@gmail.com

Abstract: *In this paper the Space Vector Pulse Width Modulation Technique is used to drive the Motor Drives by a Wind Driven Self Excitation Generator (SEIG) through an Impedance Source Inverter (ZSI). The Stand Alone application using SEIG is the most emerging application in the field of Wind Energy Conversion System (WECS). The proposed system is modelled with a generator-side Diode Bridge Rectifier and a Stand-Alone side ZSI. This employs as a bridge between the generator and the stand-alone application. The model has been simulated through MATLAB/SIMULINK using the components for Diode Bridge, Impedance Network and Induction Motor Load and the SEIG is modelled analytically. The control strategy for the proposed topology is developed from Space Vector Modulation (SVM) and Z-source Network operation principles. The maximum power from the wind turbine generator and the power is transferred to the stand alone system is achieved by adjusting the shoot-through duty cycles of the Z-source network. The performances of the SEIG based WECS has been analysed and the results are tested.*

Keywords: *Self Excited Induction Generator (SEIG), Wind Energy Conversion Systems (WECS), Impedance Source Inverter (ZSI), Space Vector Modulation Technique (SVM), Pulse Width Modulation (PWM), MATLAB, SIMULINK.*

1. Introduction:

Electrical energy is vital in every aspect of our day-to-day life. A fundamental need in the developing countries is the electrification of rural areas and remote villages. Stand-Alone Wind Electric Conversion Systems (SAWECS) [1] are a good solution to electrify isolated locations, which are far from the electrical distribution network. Due to the increasing concern about the clean environment and the depletion of natural resources such as fossil fuels and nuclear fusion materials much novel research is focused mainly on obtaining electrical power from nonconventional energy sources. Wind Energy Conversion System (WECS) are recently getting a lot of awareness, because they are cost viable, inexhaustible, environmentally clean and safe renewable energy sources compared to thermal and nuclear power generation systems. Self–Excited Induction Generator (SEIG) [12] based wind energy conversion scheme is most often installed in remote and rural villages. Induction machine working as a generator is becoming more and more popular for stand-alone wind power conversion systems. The developed solid state power electronic converters like voltage source inverter and impedance source inverter fed wind energy conversion system has facilitated the control of the output voltage of induction generators. Most of the small villages and remote areas around the world today are dependent on imported fossil fuels for most of their energy requirements. With the global awareness of the finiteness of the non-renewable resources (mainly fossil fuels) of the earth as well as the unfavourable effects they cost to our environment, people are making great effort to look for alternative sources that can provide electricity continuously while minimizing the environmental impact on the earth, which are known as renewable energy sources. Photovoltaic and wind generation schemes are considered the economic choice for small and medium scales remote area electrical energy generation.

2. Block Diagram:

In this power generation system, a horizontal axis wind turbine with a SEIG connected to the isolated load through a solid state power electronic converter [7] is considered. It consists of a wind turbine, SEIG, diode bridge rectifier, ZSI and feeding an induction motor load is shown in Fig 1. The self-excited induction generator is used in stand-alone energy conversion systems have the inherent problem of fluctuations in the magnitude and frequency of its terminal voltage with changes in wind flection and load. Hence, to overcome these difficulties an asynchronous (AC-DC-AC) link is used to interconnect the WES to the load [2].

Generally, the asynchronous link consists of a phase-controlled rectifier and a line-commutated

inverter. Each switch conducts for 120°. Only two switches remain ON at any instant of time. The output voltage and frequency of the stand-alone wind energy conversion system is vary with wind velocity; therefore a DC link converter (Rectifier and Inverter) will be used to maintain the variable voltage and variable frequency supply into fixed voltage and frequency. The inductor filter reduces the current ripple content in the DC output current and the filter capacitor reduces the ripple content in the DC link voltage providing a relatively stiff voltage source for the PWM inverter [8]. This arrangement helps in reducing the reactive power burden on the self-excitation capacitor bank since the power factor at the uncontrolled rectifier input is almost unity (neglecting the losses in the converter [7]). This helps in reducing the installed capacity of the self-excitation capacitor bank, reducing the overall cost of the system.

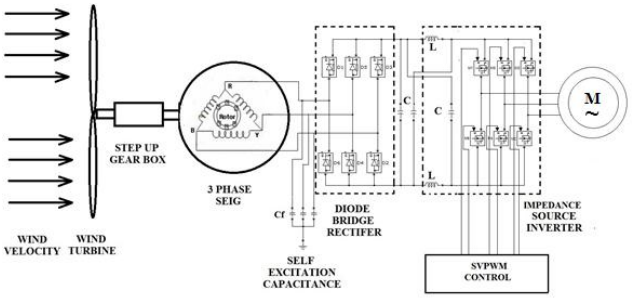

Fig. 1: Block Diagram of the Proposed Method

The ZSI is used to get constant voltage and constant frequency. The proper value of shunt capacitor of the inverter can reduces the voltage ripple content in the DC link voltage. To control output voltage of the impedance source inverter [15], the SVPWM strategies are the effective, especially describing a lower total harmonic distortion (THD). The power factor is mainly depending upon the generated voltage and the wind velocity conditions. The DC link voltage ripples in the rectifier output is filtered using shunt capacitor filter. The pulse width modulation technique is used to control the inverter output voltage and frequency. It is also affected by the EMI noise.

1. Dynamic Modelling of SEIG:

The self-excited induction generator is essentially an induction machine driven by a prime mover with capacitor connected at the stator terminals as shown in Fig 2.

The loop equations for the d-axis and q-axis equivalent circuits are,

$$r_s i_{qs} + L_s \frac{di_{qs}}{dt} + L_m \frac{di_{qr}}{dt} = V_{ds}\omega_e \quad (1)$$

$$r_r i_{qr} + L_r \frac{di_{qr}}{dt} + L_m \frac{di_{qs}}{dt} = V_{dr}(\omega_e - \omega_r) \quad (2)$$

$$r_s i_{ds} + L_s \frac{di_{ds}}{dt} + L_m \frac{di_{dr}}{dt} = -V_{ds} + V_{qs}\,\omega_e \quad (3)$$

$$r_r i_{qr} + L_r \frac{di_{dr}}{dt} + L_m \frac{di_{ds}}{dt} = V_{qr}(\omega_e - \omega_r) \quad (4)$$

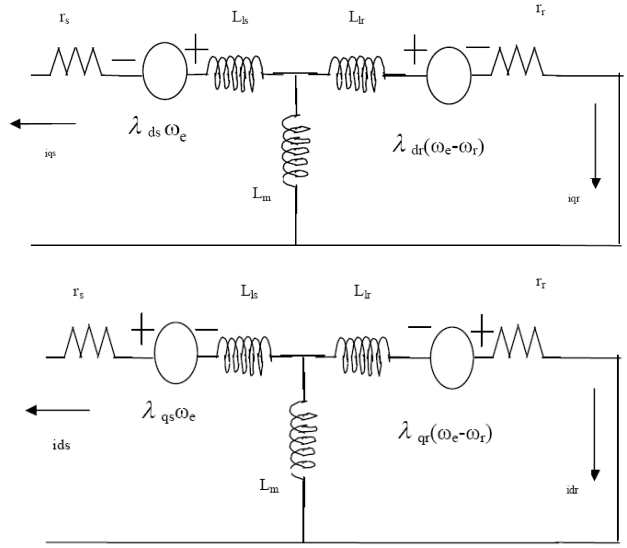

Fig. 2: Equivalent Circuit of SEIG in d-q reference frame.

The dynamics of the self-excited induction generator can be represented by the following electromechanical equations derived in the synchronously rotating d-q reference frame.

$$pi_{qs} = -K_1 r_s i_{qs} - (\omega_e + K_1 L_m \omega_r) i_{ds} + K_2 r_r i_{qr} - K_1 L_m \omega_r i_{dr} \quad (5)$$

$$pi_{ds} = -K_1 r_s i_{ds} - (\omega_e + K_2 L_m \omega_r) i_{qs} + K_2 r_r i_{dr} - K_1 L_m \omega_r i_{qr} - K_1 V_{ds} \quad (6)$$

$$pi_{qr} = K_2 L_s \omega_r i_{ds} + K_2 r_s i_{qs} + (K_1 L_s \omega_r - \omega_e) i_{dr} + [(r_r + K_2 L_m r_r] i_{qr} \quad (7)$$

$$pi_{dr} = K_2 L_s \omega_r i_{qs} + K_2 r_s i_{ds} + (K_1 L_s \omega_r - \omega_e) i_{qr} + [(r_r + K_2 L_m r_r)/L_r] i_{dr} + K_2 V_{ds} \quad (8)$$

$$pV_{ds} = \frac{i_{dc}}{c},\ \omega_e = \frac{i_{qc}}{CV_{ds}} \quad (9)$$

where

$$K_1 = \frac{L_r}{L_S L_r - L_m^2} \text{ and } K_2 = \frac{L_m}{L_S L_r - L_m^2}$$

Equations (5) - (9) are derived assuming that the d-axis is aligned with the stator terminal voltage phasor (i.e. V_{qs} = 0). In self-excited induction generators, the magnitude of the generated air-gap voltage in the steady state equation is given by,

$V_g = \omega_e L_m |i_m|$ (10)

Where,

$|i_m| = \sqrt{(i_{qs} + i_{qr})^2 + (i_{ds} + i_{dr})^2}$ (11)

$L_m = f(i_m)$

The electromagnetic torque T_g developed by the induction generator is expressed as,

$T_g = -1.5\left(\frac{Poles}{2}\right) L_m\left(i_{qs} i_{dr} - i_{ds} i_{qr}\right)$ (12)

The wind turbine and induction generator rotors are represented as a lumped mass. So the dynamic equation of motion is written as,

$p\omega_r = \left((T_t / G_r) - T_g\right) / J_g$ (13)

The developed electromagnetic torque and the torque balance equations are,

$T_e = \left(\frac{3}{2}\right)\left(\frac{P}{2}\right) L_m\left(i_{dr} i_{qs} - i_{qr} i_{ds}\right)$ (14)

$T_{shaft} = T_e + J\left(\frac{P}{2}\right) p\omega_r$ (15)

The torque balance equation is expressed in speed derivative form as,

$p\omega_r = \left(\frac{P}{2J}\right)\left(T_e - T_{shaft}\right)$ (16)

1.1. Flow Chart for Modelling Induction Generator:

The induction generator model is developed without taking core loss and hysteresis loss. The dynamic model of the induction machine can be represented by the electromechanical equations.

The flowchart of the Induction Generator is shown in the Fig. 3.

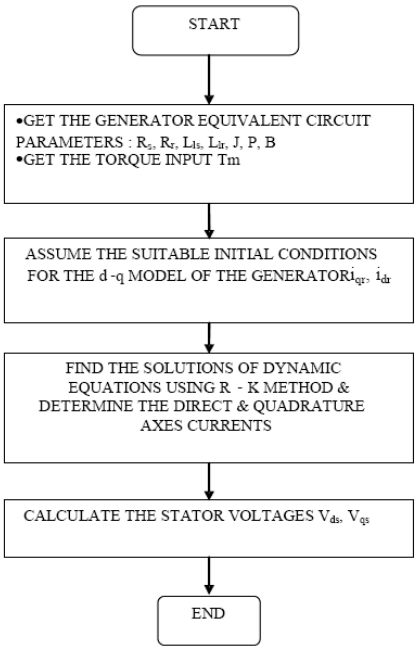

Fig. 3: Flowchart for Modelling the Induction Generator

2. Space Vector Pulse Width Modulation (SVPWM) Technique:

Space vector modulation (SVM) [14] is an algorithm for the control of pulse width modulation (PWM). It is used for the creation of alternating waveform (AC) waveform. It most commonly used in inverters, 3 phase ac powered motors. There are various types of SVM that result in different quality and computational requirements. One active area of development is in the reduction of total harmonic distortion (THD) created by the rapid switching inherent to these algorithms. With the increase of levels, traditional approaches of SVM based on five-level or seven level inverters are hardly realized. Some modified methods have been proposed to approach the SVM of inverter with any levels. One of them is carrying out the SVM in 60-degree coordinates. This section will outline this SVM scheme. Any three-phase system (defined by $a_x(t)$, $a_y(t)$ $a_z(t)$) can be represented uniquely by a rotating vector as ,

$a_s = \frac{2}{3}\left[a_x(t) + a.a_y(t) + a^2.a_Z(t)\right]$ (17)

Given a three-phase system, the vector representation is achieved by the following 3/2 transformation:

$$\begin{bmatrix} A_\alpha \\ A_\beta \end{bmatrix} = \frac{2}{3} \cdot \begin{bmatrix} 1 & \frac{-1}{2} & \frac{-1}{2} \\ 0 & \frac{\sqrt{3}}{2} & \frac{-\sqrt{3}}{2} \end{bmatrix} \cdot \begin{bmatrix} a_X \\ a_Y \\ a_Z \end{bmatrix}$$

Where (Aα, Aβ) are forming an orthogonal 2-phase system and $a_S = A_\alpha + jA_\beta$. A vector can be uniquely defined in the complex plane by these components. The reverse transformation (2/3 Transformation) is given by,

$$\begin{cases} a_X(t) = Re[a_S] + a_0(t) \\ a_Y(t) = Re[a^2.a_s] + a_0(t) \\ a_Z(t) = Re[a.a_s] + a_0(t) \end{cases}$$

$$a_0 = \frac{1}{3}.[a_X(t) + a_Y(t) + a_Z(t)]$$

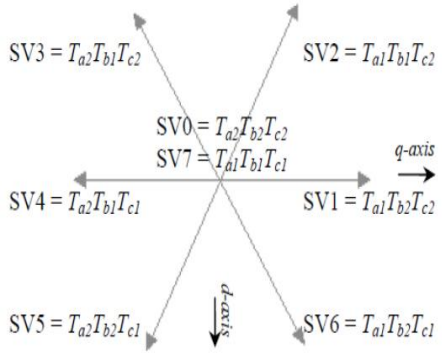

Fig. 4: Space vector d,q-axis locations and their corresponding closed switches

It represents the homopolar component. It results a unique correspondence between a Space Vector in the complex plane and a three-phase system. The method of choosing active vectors is the same regardless of which SVM algorithm is used. The Space Vector representation is shown as in Figure 4.

3. Impedance Source Inverter:

A Z-source inverter [13] is proposed as the single-stage inverter topology to demonstrate both buck and boost power conversion ability. In addition, the two switches in the same phase leg can be gated on simultaneously and no lead time is needed, so the output distortion is greatly reduced and the reliability can be improved. Impedance network is a two port network. A two port network is simply a network inside a box and the network has only two pairs of accessible terminals. Usually one pair represents the input and other represents the output. This network also called as lattice network. Lattice network is the one of the common four terminal two port network.

The lattice network is used in filter sections and is also used as attenuators. Lattice networks are sometimes used in preference to ladder structure in some special applications. This lattice network, L_1 and L_2 are series arms inductances, C_1 and C_2 are diagonal capacitances. This is a two port network that consists of split inductors L_1 and L_2 and capacitors C_1 and C_2 connected in X-shape. The impedance source inverter bridge has one extra zero state. When the load terminals are shorted through both upper and lower devices of any one phase leg or all three phase legs this shoot through zero state is forbidden in the VSI, because it would cause a shoot-through fault. This network makes the shoot through zero state possible. This state provides the unique buck-boost [8] feature to the inverter. The equivalent circuit of the Impedance Source Inverter is shown in Fig. 5. The inverter bridge is equivalent to a short circuit when the inverter bridge is in the shoot-through zero state. The equivalent switching frequency from the impedance source network is six times the switching frequency of the main inverter, which greatly reduces the required inductance of the impedance source network.

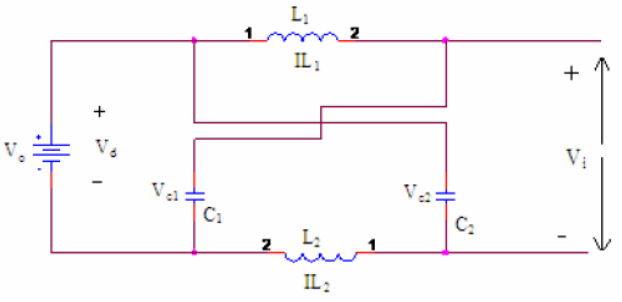

Fig. 5: Equivalent Circuit of ZSI

3.1. Mathematical Modelling of ZSI:

The three phase Z-source inverter fed load system is shown in Fig. 6. This type of inverter has a lattice network or impedance network on its DC side, which connects the source to the inverter. The two inductors and two capacitors are used to provide buck and boost operation.

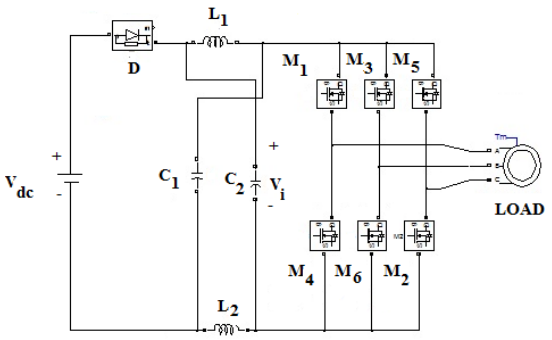

Fig. 6: Impedance Source Inverter (ZSI)

Assume the inductors (L_1 and L_2) and capacitors (C_1 and C_2) have the same inductance and capacitance values respectively.

L_1 and L_2 – series arm inductors; V_{dc} is input voltage;

C_1 and C_2 – parallel arm capacitors; V_i is output voltage;

$$V_{c1} = V_{c2} = V_c \qquad (18)$$

$V_{L1} = V_{L2} = V_L$ (19)
$V_L = V_c$
$V_D = 2V_c$
$V_i = 0$
During the switching cycle T
$V_L = V_o - V_c$ (20)
$V_D = V_o$
$V_i = V_c - V_L = 2\ V_c - V_o$
$V_i = 2V_c - V_o$ (21)
Where V_o is the DC source voltage and
$T = T_o + T_1$ (22)

The average voltage of the inductors over one switching period (T) should be zero in steady state,

$V_L = V_L = T_o * V_c + T_1 (V_o - V_c) / T = 0$
$V_L = (T_o * V_c + V_o * T_1 - V_c * T_1) / T = 0$
$V_L = (T_o - T_1) V_C / T + (T_1 * V_o) / T$
$V_c / V_o = T_1 / (T_1 - T_o)$ (23)

Similarly the average DC link voltage across the inverter bridge can be found as follows from Equation (22)

$V_i = (T_o * 0 + T_1) * (2V_c - V_o) / T$ (24)
$V_i = (2V_c . T_1/T) - (T_1 V_o/T)$
$2V_c = V_o$
From Equation (xxi)
$T_1 * V_o / (T_1 - T_o) = 2V_c * T_1 / (T_1 - T_o)$
$V_c = V_o * T_1 / (T_1 - T_o)$
The peak DC link voltage across the inverter bridge is
$V_i = V_c - V_L = 2\ V_c - V_o$
$= T / (T_1 - T_o).V_o = B * V_o$
Where B = T/ (T1-To) i.e ≥1 (25)
B is a boost factor

4. Simulation and Results:

The Matlab/Simulink model of the SEIG fed motor load through ZSI based AC to AC converter is shown in Fig.7. These input capacitors serve as the DC source feeding the Z-source network and are used to suppress voltage surge that may occur due to the line inductance during diode commutation and shoot-through mode of the inverter, thus requiring a small value of capacitance.

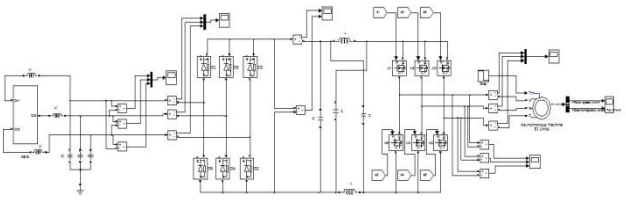

Fig. 7: Simulink Model of the Proposed System

The value of the self-exciting capacitance has to be calculated from the Synchronous Speed test.

4.1. Synchronous Speed Test:

The no load saturation curve of the machine is obtained at normal rated frequency. The voltage source is applied to the stator of the induction machine while its rotor is driven by the DC motor at a constant speed corresponding to the synchronous speed of the machine at 50Hz. It is customarily assumed that the magnetizing current is the difference between stator current and rotor current referred to the stator. In the present case the slip is very small (practically zero) which implies that the magnetizing branch current is essentially measured stator no load current. The synchronous speed test results are presented in the following Table 1.

Table 1: Synchronous Speed Test

#	Phase Voltage (V)	Magnetising Current (A)
1	0	0
2	35	0.5
3	60	0.9
4	134	1.8
5	178	2.7
6	214	3.5
7	231	3.9
8	240	4.2
9	254	5.4
10	261	6.9
11	269	7.5

The no load characteristics of the SEIG as shown in Figure 7.1. The critical capacitance is limited by the linear region of no load curve, below this value if the capacitance is chosen the voltage will never buildup and excitation fails initially. The minimum capacitance value is limited by the rated

voltage of the machine; if we choose below this value the rated voltage will not be generated. The maximum value of capacitance used is limited by the rated motor current. If a capacitance exceeds the maximum value current flow will be more than the rated current which leads to heating of stator core.

4.2. Design of Critical, Minimum and Maximum Capacitance Value:

The Maximum and the Minimum Capacitance value are calculated for the frequency, f = 50Hz as,

Critical Capacitance,

$X_{cc}=\frac{\Delta V}{\Delta I}=\frac{62}{0.97}=63.92\approx 64\Omega$

$C_{cc}=\frac{1}{2*\pi*f*X_c}=\frac{1}{2*\pi*50*64}=49.8\approx 50\mu F$

Minimum Capacitance $X_{cmin}=\frac{\Delta V}{\Delta I}=\frac{240}{4.17}=57.55\Omega$

$C_{min}=\frac{1}{2*\pi*f*X_c}=\frac{1}{2*\pi*50*57.55}=55.31\approx 55\mu F$

Maximum Capacitance $X_{cmax}=\frac{\Delta V}{\Delta I}=\frac{269}{7.5}=35.867\Omega$

$C_{max}=\frac{1}{2*\pi*f*X_c}=\frac{1}{2*\pi*50*35.87}=88.748\approx 89\mu F$

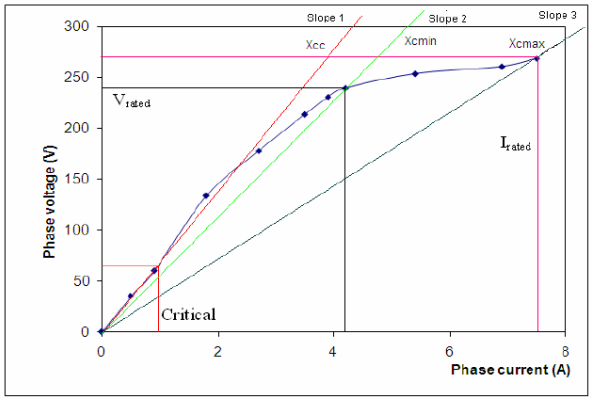

Fig. 7.1: No load characteristics of SEIG

X_{cc} - Critical capacitive reactance is limited by linear region.

X_{cmin} - Minimum capacitive reactance is limited by rated voltage.

X_{cmax} - Maximum capacitive reactance is limited by rated current.

During one switching cycle, the output filter inductor is large enough to assume that the output current is constant and is much greater than resonant inductor L_r. The capacitor C1 is large enough to assume that the voltage is constant and ripple free. Fig. 8 and 9 shows the phase voltage V_a,V_b,V_c and phase current I_a, I_b, I_c waveforms of the wind driven SEIG of the proposed system respectively. Figure 10 output line voltages V_{ab}, V_{bc} and V_{ca} at the AC motor terminal. Figure 11 and 12 shows the speed curve and Electromagnetic Torques of the motor respectively. The THD obtained for the SVM based ZSI is reduced to 3.01%.

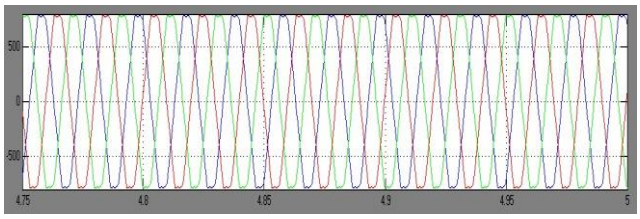

Fig. 8: Phase voltage V_a,V_b,V_c of SEIG

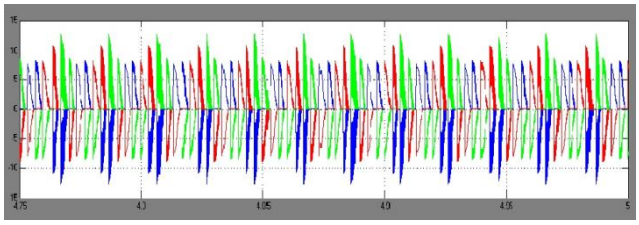

Fig. 9: Phase Current I_a, I_b, I_c of SEIG

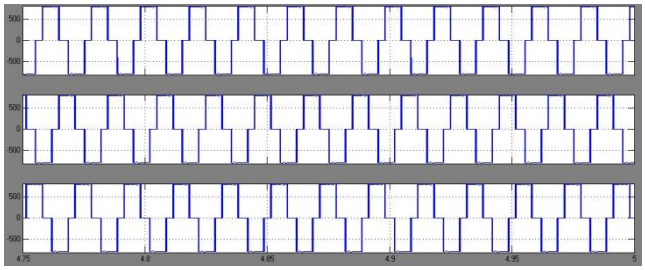

Fig. 10: Output Voltage of AC Motor

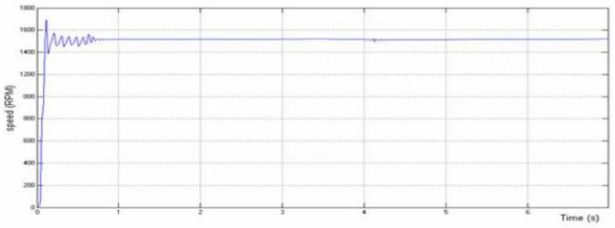

Fig. 11: Speed of the AC Motor

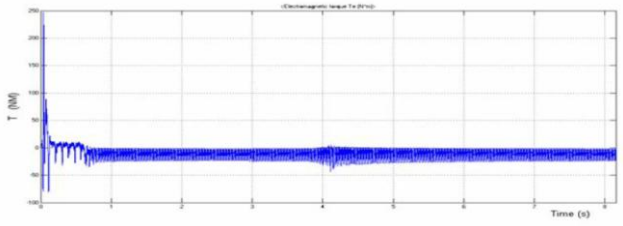

Fig. 12: Electromagnetic Torque of AC Motor

5. Experimental Setup and Results:

The 4 pole, 415 volts, 7.5 amps, 3H.P and 50Hz squirrel cage induction generator was coupled to a

separately excited D.C drive motor to provide different speeds. The prime mover can be controlled by armature rheostat of 220 ohm / 5 amps. Fig. 13 shows the photo graph of SEIG connected with the D.C separately excited motor (Prime mover). In this generator is loaded with the proper excitation capacitance. The excitation capacitance C_{cc} = 60µf connected across the terminals of the generator. As the load resistance is increased to 60Ω, the stator voltage decreases to 230 volts.

Fig. 13: Experimental Setup of the proposed system

The generator voltage can be evaluated with the varying excitation capacitance of C_{cc} = 50µf, 55µf and 60µf. The induction generator has been extensively simulated for various load conditions and varying excitation capacitances. The generated voltage of the studied SEIG is converted into DC voltage by using the diode bridge rectifier. The minimum, critical and maximum capacitance for self-excitation process in induction generator can be calculated. The wind driven SEIG performance can be analysed with the varying excitation capacitance and load resistance values. The condition for maintaining excitation is sufficient amount of capacitance connected to the motor terminals. The experimental set up is shown in Fig. 11. At no load condition, the generated voltage of the SEIG was carried for various excitation capacitance values of 50 µf, 55 µf and 89 µf. The generated voltage of 177 volts, 190 volts and 229 volts was found from the above mentioned excitation capacitances. Fig. 14 shows the experimental results of SEIG.

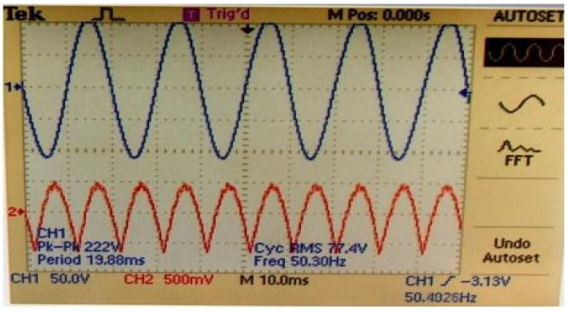

Fig. 14: Experimental result of SEIG with load R=60Ω per phase (a) Terminal Voltage 50 V/div. (b) DC link Voltage 103V/div.

6. Conclusion:

The proposed work demonstrated the state of art AC-DC-AC power converter technology. The mathematical analysis of the impedance source inverter is developed. The analysis and simulation of a SEIG driven by a wind turbine is carried out to study its performance as a stand - alone power supply. A DC link converter is introduced in the WECS model, and the effect of modulation index on the generated power is studied for a given wind velocity and load. The simulation results are in line with the predictions.

The performance of Z – source inverter for SEIG fed wind energy conversion system has been proposed and corresponding simulated waveforms are verified. The output voltage of the Z – source inverter is entirely depends upon the shoot through states. The impedance source inverter based stand-alone wind energy conversion system is simulated and its performance is analysed by varying the load values. The hardware is tested and the results are presented. The experimental results coincide with the simulation results. A detailed performance analysis of stand-alone wind energy conversion system is made.

Reference:

1. Hua Geng, Dewei (David) Xu, Bin Wu and Wei Huang, "Direct Voltage Control for a Stand-Alone Wind-Driven Self-Excited Induction Generator with Improved Power Quality," IEEE Transactions on Power Electronics, vol. 26, no. 8, August 2011. pp. 2358 – 2368.
2. Sholi Nishikata and Fujio Tatsuta, "A New interconnection Method for Wind Turbine/Generator in a Wind Farm and basic Performances of the Integrated System," IEEE Transactions on Industrial Electronics, vol. 57, no. 2, February 2010. pp. 468-475.
3. Z. Chen, J. M. Guerrero, and F. Blaabjerg, "A review of the state of the art of power electronics for wind turbines," IEEE Transactions of Power Electronics, vol. 24, no. 8, Aug. 2009. pp. 1859–1875.
4. J. M. Carrasco, L. G. Franquelo, J. T. Bialasiewicz, E. Galvan, R. C. P. Guisado, A. M. Prats, J. I. Leon, and N.Moreno-Alfonso," Power Electronic systems for the grid integration of renewable

energy sources: A survey," IEEE Transactions of Industrial Electronics, vol. 53, no. 4, Aug. 2006, pp. 1002–1016.
5. A. Mirecki, X. Roboam, and F. Richardeau, "Architecture complexity and energy efficiency of small wind turbines," IEEE Transactions of Industrial Electronics, vol. 54, no. 1, Feb. 2007,pp. 660–670.
6. P. Rodriguez, A. V. Timbus, R. Teodorescu, M. Liserre, and F. Blaabjerg, "Flexible active power control of distributed power generation systems during grid faults," IEEE Transactions of Industrial Electronics, vol. 54, no. 5, Oct. 2007, pp. 2583–2592.
7. J. F. Conroy and R. Watson, "Low-voltage ride-through of a full converter wind turbine with permanent magnet generator," IET Renewable Power Generation, vol. 1, no. 3, Sep. 2007, pp. 182–189.
8. M. Malinowski, S. Stynski, W. Kolomyjski, and M. P. Kazmierkowski, "Control of three-level PWM converter applied to variable-speed-type turbines," IEEE Transactions of Industrial Electronics, vol. 56, no. 1, Apr. 2009,Jan 2009, pp. 69-77.
9. J. A. Sayago, T. Bruckner, and S. Bernet, "How to select the system voltage of MV drives - A comparison of semiconductor expenses," IEEE Transactions of Industrial Electronics, vol. 55, no. 9, pp. Sep.2008, 3381–3390.
10. T. Nussbaumer, M. Baumann, and J.W. Kolar, "Comprehensive design of a three-phase three-switch buck-type PWM rectifier," IEEE Transactions of Power Electronics, vol. 22, no. 2, Mar. 2007, pp. 551–562.
11. M. Baumann and J. W. Kolar, "Parallel connection of two three-phase three-switch buck-type unity power-factor rectifier systems with DC link current balancing," IEEE Transactions of Industrial Electronics, vol. 54, no. 6, Dec. 2007, pp. 3042–3053.
12. Sasikumar M. and Chenthur Pandian S. (2011), 'Modeling and Analysis of Cascaded H-Bridge Inverter for Wind Driven Isolated Self – Excited Induction Generators,' International Journal on Electrical Engineering and Informatics (IJEEI), Vol.3, No. 2, 2011, pp. 132-145.
13. Sasikumar M. and Chenthur Pandian S. (2010), 'Implementation of an impedance source inverter based variable speed wind driven self - excited induction generator,' Journal of Electrical Engineering (JEE), Vol.10, No.3, pp. 43 – 47.
14. F. Max Savio, S. Vasantharaj and M. Sasikumar (2012), "Implementation of Stand-Alone Hybrid System using SVPWM for Impedance Source Inverter", Wulfenia Journal, vol. 19, no. 11, pp. 404-417.
15. F. Max Savio and M. Sasikumar (2012), "Space Vector Control Scheme of Three Level ZSI Applied to Wind Energy Systems", International Journal of Engineering, IJE Transaction C: Aspects, vol. 25, no. 4, pp. 275-282.

Author's Biography:

Mr. F. Max Savio has received the Bachelor Degree in Electrical and Electronics Engineering from Jeppiaar Engineering College, Anna University, India in 2007. He has worked four years with Essar Projects [India] Limited in Electrical and Instrumentation Material Testing, Field Erection and Material Procurement. He is pursuing Master of Engineering in Power Electronics and Drives from Jeppiaar Engineering College, Anna University, India. His area for interest includes in the field of Wind Energy Systems, Power Converters and PWM techniques.

Mr. S. Vasantharaj has received the Bachelor degree in Electrical and Electronics Engineering from M. Kumarasamy College of Engineering, Anna University, India in 2008. He has worked one year for Gulfmax International LLC, Dubai and one year for LMD Electricals and Engineering works, India in Electrical Maintenance. He is pursuing Master of Engineering in Power Electronics and Drives from Jeppiaar Engineering College, Anna University, India.

Dr. M. Sasikumar has received the Bachelor degree in Electrical and Electronics Engineering from K.S.Rangasamy College of Technology, Madras University, India in 1999, and the M.Tech degree in power electronics from VIT University, in 2006. He has obtained his Ph.D. degree from Sathyabama University, Chennai. Currently he is working as a Professor and Head of Department of Electrical and Electronics Engineering in Jeppiaar Engineering College, Chennai Tamilnadu, India. He has published papers in National, International conferences and journals in the field of power electronics and wind energy conversion systems. His area of interest includes in the fields of wind energy systems and power converter with soft switching PWM schemes. He is a life member of ISTE.